RESEARCH PAPER

PCCP
www.rsc.org/pccp

Ring currents in large [4*n* + 2]-annulenes†

Alessandro Soncini,*[a] Patrick W. Fowler[a] and Leonardus W. Jenneskens[b]

[a] *School of Chemistry, University of Exeter, Stocker Road, Exeter, UK EX4 4QD. E-mail: A.Soncini@exeter.ac.uk and P.W.Fowler@exeter.ac.uk; Fax: +44 1392 263434*

[b] *Debye Institute, Department of Physical Organic Chemistry, Utrecht University, Padualaan 8, 3584 CH, Utrecht, The Netherlands. E-mail: jennesk@chem.uu.nl; Fax: +31 30 2534533*

Received 19th September 2003, Accepted 14th October 2003
First published as an Advance Article on the web 31st October 2003

Reported computational results for large [4*n* + 2]-annulenes indicate a falling off of aromaticity in D_{3h} geometries but its retention in D_{6h} geometries, as diagnosed on both energetic and magnetic criteria. Ipsocentric pseudo-π mapping of the current density induced by a perpendicular external magnetic field shows that ring currents follow this trend. Diatropic ring currents are quenched in D_{3h} geometries but survive in D_{6h} geometries of [4*n* + 2]-annulenes (4*n* + 2 = 30, 42, 54, 66). Ipsocentric orbital contributions explain this distinction in terms of the translational/diatropic, rotational/paratropic selection rules for current in monocycles, coupled with an account of differential angular-momentum mixing in D_{3h} and D_{6h} symmetries. The orbital model rationalises the differences between D_{6h} and D_{3h} geometries, accounts for the decay of aromaticity with ring size for D_{3h} [4*n* + 2]-annulenes, and predicts trends for anti-aromatic [4*n*]-annulenes in the two symmetry groups.

Introduction

Implicit in even the simplest molecular orbital approaches to cyclic π-conjugated systems is the prediction that the electronic and geometric structures of [*n*]-annulenes should result from a compromise between the inherent localising tendency of π electrons and the delocalisation imposed by the σ framework. As the system size increases, so does the energetic benefit of localisation.[1–3] Recent calculations on large [4*n* + 2]-annulenes[4–6] predict a falling off in aromatic character with increasing ring size, beyond a threshold of $n \sim 7$, *i.e.* from [30]-annulene onwards.

The evidence presented in ref. 4 is based on energy, geometry and magnetic response. For the series $C_{30}H_{30}$, $C_{42}H_{42}$, $C_{54}H_{54}$, $C_{66}H_{66}$, computed aromatic stabilisation energies for D_{3h} structures tend to a constant value of ~ 92 kJ mol^{-1} per molecule and hence, counted per electron, to a decreasing contribution of π aromatic delocalisation to stability. This trend accompanies increasing geometric localisation, again with an onset, according to DFT calculations, at [30]-annulene. Hartree–Fock calculations on the same systems exhibit a greater degree of localisation for all annulenes beyond benzene itself and would place the threshold of geometric localisation much earlier[4] but agree with DFT in the general trends.

Magnetic properties in this series also indicate progressive loss of aromaticity beyond $C_{30}H_{30}$, with a predicted downward trend in the magnitudes of diamagnetisability exaltation, nucleus-independent chemical shift at ring centres (NICS(0)) and in the differential chemical shifts between internal and external hydrogen nuclei. In contrast, in specially constructed DFT geometries where greater uniformity of bond length is imposed by D_{6h} symmetry constraints, the annulenes $C_{30}H_{30}$ to $C_{66}H_{66}$ show a rising trend in the magnitudes of all these magnetic indices.

Given the widely accepted definition of aromaticity as the ability of a system to sustain a diatropic ring current,[7–9] these systematic variations in computed magnetic properties should have implications for the underlying ring currents of large [4*n* + 2]-annulenes. In particular, we could expect from the values of NICS(0) that, insofar as this quantity can be taken as an index of ring current strength, ring current should fall off with increasing ring size for the D_{3h}, but should grow stronger with increasing size for the D_{6h} geometries of the [4*n* + 2]-annulene systems.

These intuitive expectations give the starting point for the present paper, as the behaviour that they predict is qualitatively different from what is known of the theory of ring currents in small [4*n* + 2]-annulenes.

For small monocycles in symmetrical planar geometries, simple Hückel theory gives a clear prediction for the sense of ring current density,[10] one that is based on the ipsocentric[11] theory of orbital contributions. These contributions arise solely from occupied-to-virtual excitations and give rise to diatropic and paratropic current accordingly as their symmetry product matches that of an in-plane translation or rotation, respectively. In the pure Hückel model a [4*n* + 2]-π system in full $D_{(4n+2)h}$ symmetry should sustain a diatropic ring current arising entirely from the four-electron HOMO–LUMO excitation; a [4*n*]-π system in the D_{2nh} symmetry compatible with closure of the π shell should sustain a paratropic ring current arising from the two-electron HOMO–LUMO excitation.

This simple picture survives essentially unchanged in the *ab initio* ipsocentric treatment of 6 π and 8 π systems and is the basis for description of geometric effects in aromaticity of clamped systems.[12] How is it to be reconciled with the reported results of computations on the larger systems?

In the present note we consider the effect of symmetry lowering from $D_{(4n+2)h}$ to D_{6h} and D_{3h} and show that the ipsocentric orbital model can indeed account for the computational result of decreasing aromaticity in large annulenes of low symmetry. For this purpose, we apply the recently developed[13] pseudo-π approach to visualise directly the ring currents in the [4*n* + 2]-annulene series.

† Presented at the ESF Exploratory Workshop: New Perspectives on Aromaticity, Exeter, UK, July 5–9, 2003.

DOI: 10.1039/b311487b

Method

(i) The ipsocentric approach

In the ipsocentric approach to calculation of current density induced by an external magnetic field, the origin of vector potential for the current density at a given point in space is taken to be the point itself. This simple *ansatz*, which is the logical limit of various strategies for distribution of origin that have been used to improve calculated results in previous work,[14–16] avoids the difficulties of gauge dependence exhibited by single-centre, finite-basis calculations, and produces physically realistic current-density maps,[10] even with the relatively modest 6-31G** basis set. The approach was first introduced by Keith and Bader[17] under the acronym CSGT (continuous set of gauge transformations), and implemented as an analytic coupled Hartree–Fock procedure by Lazzeretti, Zanasi and co-workers[18,19] under the acronym CTOCD-*DZ* (continuous transformation of origin of current density-*diamagnetic zero*). The two descriptions 'diamagnetic zero' and 'ipsocentric' are equivalent: choice of a point as its own origin of vector potential formally removes the diamagnetic component of current density at that point.

In the ipsocentric treatment, the traditional separation of magnetic response into diamagnetic and paramagnetic terms is replaced by a partition of the first-order wave-function into two excited-state sums,[10] involving respectively linear momentum and angular-momentum operators, and hence governed in the one case by translational and in the other case by rotational selection rules. Consideration of frontier-orbital energies and symmetries leads to a readily applied physical model for orbital contributions to ring currents,[10,11] free of the complications introduced in other approaches by non-physical occupied-to-occupied mixing terms.

(ii) The pseudo-π model

It was pointed out recently that, in the special case of the π currents induced in planar polycyclic hydrocarbon systems, it is possible to duplicate the main features of the full *ab initio* calculation by a simplified 'pseudo- π' procedure at much lower computational cost.[13] In a pseudo- π treatment of a carbocyclic system, the carbon centres of the conjugated skeleton are retained, each bearing a single 1s basis function, and all other atoms are deleted. An ipsocentric calculation of current *in the plane* of the atomic centres is then carried out.

It turns out that when the pseudo-π basis functions are chosen as hydrogenic STO-3G 1s orbitals, the computed in-plane σ current matches closely the true current calculated for the full π system of the original hydrocarbon at the usual height of $1a_0$ above the plane. As the basis consists now of only one function per carbon centre, there is a huge saving in computational cost, without significant loss of information about π currents.

The theory of the pseudo-π method relies on the one-to-one match between in-plane σ orbitals of the set of pseudo-hydrogen atoms and the out-of-plane π orbitals of a full system with the same connectivity (each σ combination becomes equisymmetric with one of the π combinations on multiplication by the symmetry of the out-of-plane vector). This analogy between π systems and clusters of hydrogen atoms was noted as long ago as 1937 by London.[20] The new observation was that this old model could be given *numerical* accuracy by appropriate choice of exponent and by using the ipsocentric approach.

The coincidence extends to the magnitude, sense, orbital decomposition and even the geometry dependence of the model current and the true π ring current.[13] Crucially, the pseudo-π method retains the ipsocentric choice of origin of vector potential, the feature of the full *ab initio* method that leads to physically realistic orbital contributions which obey symmetry-based selection rules.

Ref. 13 details tests of the pseudo-π method on systems with up to 26 conjugated carbon atoms; the method has also been used for a 36-atom conjugated system within a fluorofullerene 'trannulene' cage, where it gave currents in good agreement with full *ab initio* calculations,[21] and in unpublished work on larger graphitic flakes, where it again captures the essentials of the π current map. It is expected to perform well in the size range required here. We therefore use the pseudo-π method in the present application as ideally suited to semi-quantitative treatment of large planar π systems. Given a model, experimental, or a computed geometry, ring-current maps can be obtained economically for systems with hundreds of atoms.

Calculations

In the present calculations, the geometries of the series of $[4n+2]$-annulenes were taken without change from ref. 4 (see supplementary material at http://pubs.acs.org/) where the geometries were optimised (under planar symmetry constraints[22]) at both Hartree–Fock (HF) and density-functional (DFT) levels using the 6-31G* basis and B3LYP functional. The reported lowest energy structures have point-group symmetries at DFT (HF) levels as follows: C_6H_6 D_{6h} (D_{6h}), $C_{10}H_{10}$ C_{2v} (C_s), $C_{14}H_{14}$ D_{2h} (C_{2v}), $C_{18}H_{18}$ D_{6h} (D_{3h}), $C_{22}H_{22}$ D_{2h} (C_{2v}), $C_{26}H_{26}$ D_{2h} (C_{2v}), $C_{30}H_{30}$ D_{3h} (D_{3h}), $C_{42}H_{42}$ D_{3h} (D_{3h}), $C_{54}H_{54}$ D_{3h}(D_{3h}), $C_{66}H_{66}$ D_{3h} (D_{3h}). For the smaller molecules in the set, these represent fully characterised minima, for the largest they apparently represent the best planar structures.[22] For the larger systems ($4n+2 \geq 30$) D_{6h}-constrained DFT structures are also given in ref. 4; these are models for geometries with reduced bond alternation. The computed energy differences between D_{3h} and these constrained D_{6h} systems are small (only 0.26 kJ mol^{-1} for [30], growing to 25.5 kJ mol^{-1} for [66][4]). A pseudo-π calculation of the ring current was performed at each geometry, and molecular-orbital contributions obtained. The results were plotted as current-density maps.

Results

We discuss first the results of current density mapping based on DFT geometries. As we will see later, the HF geometries give similar results but with a much earlier onset of those features that can be ascribed to localisation.

For the $[4n+2]$-annulenes with fewer than 30 carbon centres, the results with DFT geometries were in agreement with expectation both from the simple Hückel model and the deductions from the reported trends in NICS(0).[4]

In this size range, each system exhibits a diamagnetic ring current, in line with the large and negative NICS(0) value, and that current is overwhelmingly dominated by the contribution of the four electrons in the degenerate or near-degenerate HOMO pair, as expected from the Hückel model. As an example of the results in this range of ring size, Fig. 1 shows maps for the [18]-annulene system at the reported D_{6h} DFT geometry. In [18]-annulene there is a strong diamagnetic (diatropic) circulation with a maximum strength of $j_{max} = 0.181$ au (*cf.* 0.079 au for the pseudo-π model of benzene, and also for the real benzene π system, in the 1 a_0 plotting plane[13]). It is seen that the total π current, as modelled in the pseudo-π method, is reproduced essentially exactly by the contribution of the HOMO electrons. The remaining 14 π electrons do not contribute to the global ring current. These observations are fully compatible with the Hückel model.

However, when the maps for larger systems are examined, qualitative differences from those for the small rings begin to appear at a size of around 30 carbon centres (DFT geometries), *i.e.* at the threshold suggested by the computational

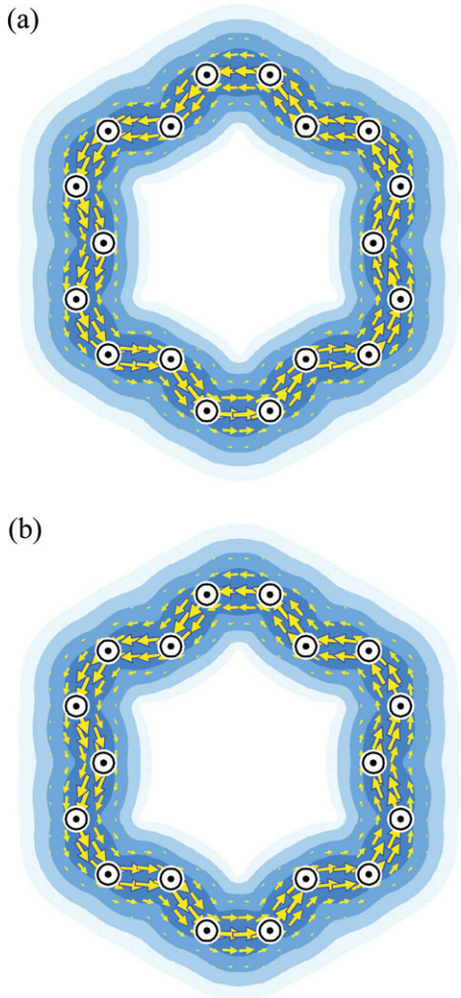

Fig. 1 Contributions to the ring current of [18]-annulene (D_{6h} DFT geometry[4]) from (a) the set of π orbitals (b) the π HOMO alone. Currents induced by a perpendicular magnetic field are computed within the pseudo-π model, and plotted using vectors to represent the current density and contours for its modulus. Anti-clockwise circulations represent diatropic currents.

evidence of ref. 4. Strikingly different patterns emerge for D_{3h} and D_{6h} series.

(i) D_{3h} geometries

First, we consider the results for the set of D_{3h} geometries for $C_{30}H_{30}$,...,$C_{66}H_{66}$, as illustrated by the composite maps shown in Fig. 2. The total current (Fig. 2c) drops rapidly in strength along the series. At $C_{30}H_{30}$ there is a still noticeable diamagnetic (diatropic) circulation with maximum strength $j_{max} = 0.044$ au, *i.e.* over half the strength of the benzene current. For the three later members of the series, this global circulation is absent and the induced current breaks up into a set of localised diamagnetic eddies associated with the set of shorter bonds of the ring ('double bonds' of the preferred Kekulé resonance structure that is implied by the bond alternation in the geometry). Indeed, the reduction of current in the later members of the series is so severe that it is necessary to increase the size of the current density arrows in order to have a usable map; the arrows in Fig. 2 are scaled by a factor of seven with respect to those in Figs. 1 and 3.

Furthermore, the orbital contributions to the total current change dramatically along the series. For the smaller $[4n+2]$-annulenes, the degenerate HOMO pair of orbitals contributes a significant diatropic global current, as noted earlier. In contrast, in $C_{30}H_{30}$ the HOMO current has a low intensity

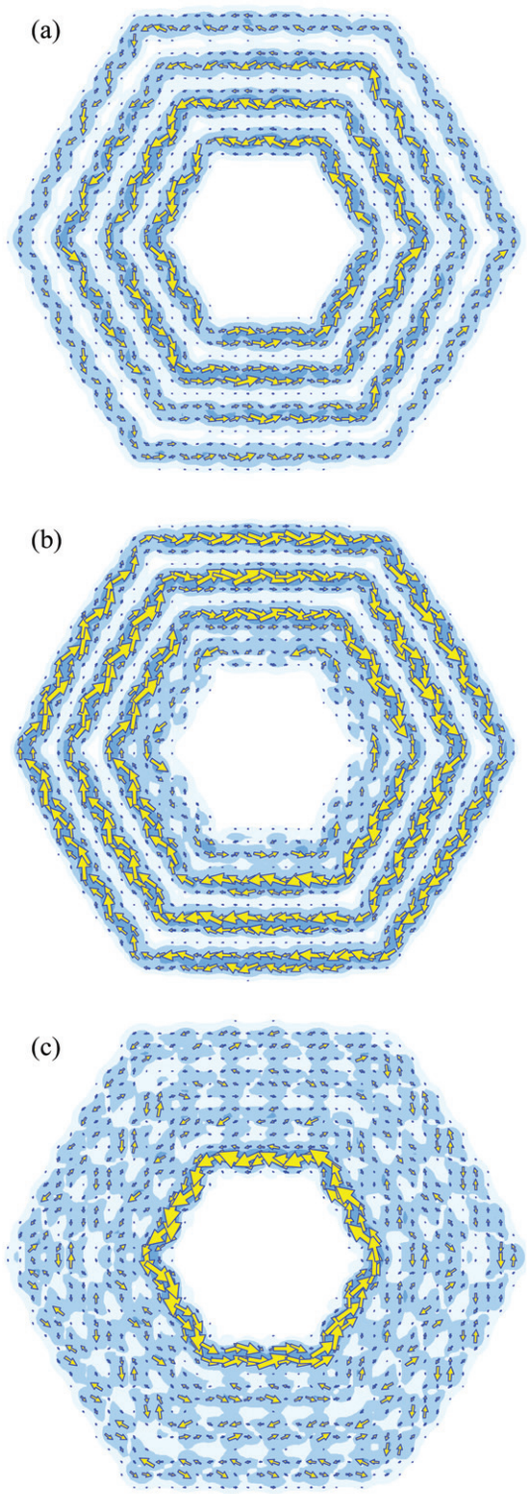

Fig. 2 Composite maps showing orbital contributions to the π ring currents in [30], [42], [54], [66]-annulenes (D_{3h} DFT geometries[4]), arranged concentrically for ease of comparison. Contributions from (a) the HOMO − 1 pair of π orbitals (b) the π HOMO pair, (c) the full set of π orbitals. Note cancellation of diatropic ring current in the three largest systems. Plotting conventions as in Fig. 1 apart from scale (see text).

($j_{max} = 0.028$ au), and by $C_{42}H_{42}$ has reversed in sense, so that the HOMO contribution is actually *paratropic* in the rest of the series. There is some indication of a maximum in the paratropic current in the range of 42 to 54 carbons (Fig. 2b). In addition, the two near-degenerate HOMO − 1 orbitals, which are unimportant in the magnetic response of smaller

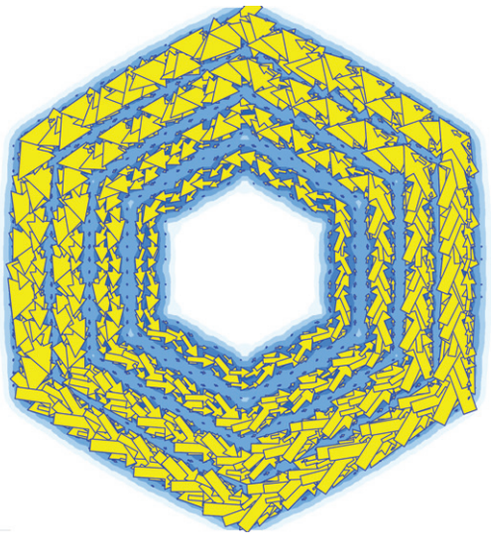

Fig. 3 Composite maps showing the π ring currents in [30], [42], [54], [66]-annulenes (D_{6h} DFT geometries[4]), arranged concentrically for ease of comparison. Contributions from the full set of π orbitals are shown, but the maps for the contributions of HOMO pairs alone would be visually indistinguishable from these. Note retention of large diatropic ring current in all systems. Plotting conventions and scale as in Fig. 1.

$[4n+2]$-annulenes at the DFT geometries, begin to make significant *diatropic* contributions at $C_{30}H_{30}$ and $C_{42}H_{42}$, before decreasing again at larger ring size. Thus, neither the total π current, nor its orbital breakdown, are as expected from the cylindrically symmetric Hückel model for a regular $[4n+2]$-gonal monocycle.

All the trends observed for the DFT geometries occur in the maps for the HF geometries, but with an earlier onset. In general, the total π currents in the HF geometries are weaker, and the loss of a global ring current occurs between 18 and 22 carbon centres; $C_{18}H_{18}$ (HF) still has a weak global circulation ($j_{max} = 0.036$ au), but in $C_{22}H_{22}$ (HF) the π current has broken up into localised islands. Decrease and reversal of the diatropic HOMO pair contribution, and growth of a diatropic contribution for the HOMO − 1 pair are also observed at this size. Thus, cases $C_{18}H_{18}$ (HF) and $C_{30}H_{30}$ (DFT) play similar pivotal rôles in their respective series, and it can be expected that the same qualitative explanation of the trends will apply to both series, once this threshold shift is taken into account.

(ii) D_{6h} geometries

Turning now to the maps for the D_{6h}-constrained DFT geometries (Fig. 3), we see a reversion to a classical Hückel pattern of diamagnetic ring currents. Currents are large and increase in strength as the size of the ring increases (and the HOMO–LUMO gap decreases). In fact, the maximum currents (j_{max}/au = 0.296 ([30]), 0.414 ([42]), 0.531 ([54]), 0.645 ([66])) show the linear increase with atom count that is expected for $[4n+2]$ systems in simple Hückel theory, where resonance energy and reduced ring current are linked.[23] The trend in computed NICS(0) values for these D_{6h} systems is less marked (−16.2 [30] −16.7 [42] −17.0 [54] −17.1 ppm [66][4]). The HOMO pair of orbitals dominates the total current-their contribution is not mapped separately here as it is indistinguishable from the total current on the present scale. Clearly, the dichotomy between maps for D_{3h} and D_{6h} geometries, and the divergence of the D_{3h} maps from the expectations of the naive orbital model require an explanation. The following section will provide this.

Discussion

Our mapping calculations have shown that the qualitative differences in magnetic properties between small and large $[4n+2]$-annulenes can be attributed to changes in the underlying induced current density, and that these changes can be reproduced by a procedure as simple as the pseudo-π method. The pseudo-π currents are consistent with the bimodal patterns of magnetisabilities, ^{1}H NMR shifts and NICS(0) values computed with sophisticated DFT techniques. Given that such a simple calculation exhibits the correct trends in ring current, it seems that it should also be possible to give a qualitative explanation for these trends.

A natural starting point is Hückel theory, where it has been shown that predictions for ring currents in small $[4n+2]$-annulenes can be made successfully on the basis of angular-momentum arguments.

(i) Angular-momentum symmetry

As is well known,[24] in the simplest version of the Hückel model, the N orbital energies ε_k for a ring of N atoms, all with equal Coulomb integrals α and connected by bonds and equal resonance integrals β for all bonds, are given by

$$\varepsilon_k = \alpha + \lambda_k\beta, \qquad (1)$$

where λ_k is an eigenvalue of the adjacency matrix of the cycle,

$$\lambda_k = 2\cos(2\pi k/N) \qquad (2)$$

and the quantum number k takes values

$$0, \pm1, \pm2, \pm(N-1)/2,$$

for odd cycles, and

$$0,\ \pm1, \ldots, \pm(N-2)/2, +N/2$$

for even cycles. Levels with equal and opposite k values are degenerate and correspond to the ± components of angular momentum about the principal axis.

The eigenvalues span the range from $\lambda_0 = +2$ for the most bonding orbital to $\lambda_{N/2} = -2$ or $\lambda_{(N-1)/2} > -2$ for the most antibonding. They are also easily found from the Frost–Musulin[25] construction, where energies correspond to the vertex heights of an N-gon inscribed point-down in a circle of radius 2β. Closed-shell configurations occur at the aromatic counts of 2,6,10,...,$4n+2$ π-electrons, and, in the same approximation, open shells with two electrons in two degenerate orbitals at anti-aromatic counts 4, 8,...,$4n$.

The molecular-orbital coefficients describing the contribution of the basis function on centre r, to the molecular orbital k can be chosen to be real by taking sin/cos combinations of angular momentum functions, *i.e.*

$$c_r^{(+|k|)} = \sin(2\pi|k|r/N),$$
$$c_r^{(-|k|)} = \cos(2\pi|k|r/N) \qquad (3)$$

with ($r = 1,\ldots,N$).

For $k = 0$ in all cycles, and for the most anti-bonding orbital in an even cycle, the cosine combination only is non-null.

These well known results follow from the graph theory of the cycle and are independent of the details of the basis: the dimensionless eigenvalues λ_k are the same for the basis of s functions used in the pseudo-π method and for the p orbitals of the usual Hückel π treatment.

(ii) Point-group symmetry

In applications to real molecules, it is useful to classify the orbitals in terms of point group symmetry. The assumptions of equality for all α integrals and all β integrals made in the

simple Hückel model amount to an assumption of full D_{Nh} symmetry for the planar molecular system.

In the parent cylindrical group, orbital angular momentum labels and their irreducible representations are connected in a one-to-one fashion. For $k = 0, \pm1, \pm2, \ldots$, the σ functions have symmetries

$$\Sigma_g^+/A_{1g},\ \Pi_u = E_{1u},\ \Delta_g = E_{2g},\ \Phi_u = E_{3u},\ \Gamma_g = E_{4g},\ \ldots$$

The π symmetries are found by multiplying each σ symmetry by Σ_u^+, the representation of translation along the principal axis; the π functions have symmetries

$$\Sigma_u^+/A_{1u},\ \Pi_g = E_{1g},\ \Delta_u = E_{2u},\ \Phi_g = E_{3g},\ \Gamma_u = E_{4u},\ \ldots^{26}$$

Thus, in both full and pseudo-π approaches, orbitals with different $|k|$ belong to different irreducible representations and each pair of orbitals with angular momentum components $\pm k$ spans a distinct doubly degenerate irreducible E-type representation.

Given the simple inter-conversion of π and pseudo-π orbitals, repetition in the ensuing discussion of currents and maps can be avoided by discussing only π orbitals and their symmetries, taking as understood the equivalent statements in the pseudo-π approach.

On descent to the maximal point group appropriate to a finite N cycle, D_{Nh}, the correspondence between angular-momentum and irreducible-symmetry labels is preserved within the valence space of the Hückel orbitals: each energy eigenvalue corresponds to a distinct irreducible representation of D_{Nh}. When N is odd, all $\pm k$ pairs ($k \neq (N-1)/2$) span distinct E-type representations as before. When N is even, all the $\pm k$ pairs with $k < N/2$ also span distinct E-type representations. The final pair ($k = \pm N/2$) for even N splits into two B-type non-degenerate representations, one for the most anti-bonding orbital and one for its absent rotational partner.[26]

Thus, for example, in D_{6h} benzene, the π orbitals with energies $\alpha+2\beta, \alpha+\beta, \alpha+\beta, \alpha-\beta, \alpha-\beta, \alpha-2\beta$ span A_{1u}, E_{1g}, E_{2u} and B_{1g}; the hexagon vertices lie on nodal planes of the sine function of the ±3 pair, so that the B_{2g} symmetry is not present with its B_{1g} symmetry partner in the valence space.

(iii) Symmetry and currents

This rigid correspondence of point-group symmetry and angular momentum is the basis of the four-electron rule for ring currents in $[4n+2]$ systems. When N is $4n+2$, all angular momentum shells up to $|k| = n$ are filled, and all shells with higher $|k|$ are empty. The linear momentum operators responsible for diatropic transitions in ipsocentric theory[10] transform as in-plane translations of E_{1u} symmetry in D_{Nh}, and the relevant angular momentum operator transforms as the A_{2g} rotation about the principal axis. As translationally allowed transitions obey $\Delta k = \pm1$, and rotational transitions can only mix k with $-k$, the allowed occupied-to-virtual transitions in D_{Nh} are solely those from HOMO to LUMO, and the ring current in $[4n+2]$ systems therefore arises entirely from the diatropic contribution from the four HOMO electrons.[11]

The four-electron rule applies rigorously in the maximal point group, but as we have seen, the larger $[4n+2]$-annulenes do not belong to this point group. In planar geometries, they show symmetry reduction from D_{Nh} to D_{3h}. *A key question for the discussion of their aromaticity is then the effect of this symmetry lowering on the orbitals and on ring-current selection rules.*

(iii) Symmetry reduction

Consider a geometry of the N monocycle where the point-group symmetry has been lowered from the full D_{Nh} group to D_{Mh}, where M is a divisor of N and D_{Mh} is a subgroup of D_{Nh}. The N independent π functions of the monocycle can be classified according to the irreducible representations of the lower group. Under this classification, functions with different angular momentum quantum numbers, which had distinct symmetries in the higher group, may become equisymmetric in the lower.

In the present case, for the $[4n+2]$-annulenes $C_{30}H_{30}$ to $C_{66}H_{66}$ in the structures taken from ref. 4, we are particularly interested in two subgroups of D_{Nh}. These are D_{6h}, where the angular momentum values $6m \pm p$ for a given parameter $p = 0,1,2,3$ share a common representation, and D_{3h}, where the common representations appear at the angular momentum values $3m \pm p$ (Table 1).[26]

Inverting these results, it is seen that the π orbitals of a D_{3h} or D_{6h} [N]-annulene are in general mixtures of angular momentum states, with specific restrictions on the values of k that can occur together. The two cases are now treated in turn.

D_{6h} symmetry

In D_{6h}, the possible π symmetries are those irreducible representations with a negative character under the σ_h operation, *i.e.* A_{1u}, A_{2u}, B_{1g}, B_{2g}, E_{1g}, E_{2u}. Functions with these symmetries can mix angular momentum components $|k|$ as:

$$\begin{aligned}
A_{2u}:&\quad 0,\ 6,\ 12,\ 18,\ 24,\ \ldots\\
A_{1u}:&\quad 6,\ 12,\ 18,\ 24,\ 30,\ \ldots\\
B_{1g},\ B_{2g}:&\quad 3,\ 9,\ 15,\ 21,\ 27,\ \ldots\\
E_{1g}:&\quad 1,\ 5,\ 7,\ 11,\ 13,\ \ldots\\
E_{2u}:&\quad 2,\ 4,\ 8,\ 10,\ 14,\ \ldots
\end{aligned}$$

The stack of π levels ordered by increasing node count becomes

$$\begin{aligned}
&A_{2u},\ E_{1g},\ E_{2u},\ (B_{1g}+B_{2g}),\ E_{2u},\ E_{1g},\ (A_{1u}+A_{2u}),\\
&E_{1g},\ E_{2u},\ (B_{1g}+B_{2g}),\ E_{2u},\ E_{1g},\ (A_{1u}+A_{2u}),\\
&E_{1g},\ E_{2u},\ (B_{1g}+B_{2g}),\ \ldots
\end{aligned}$$

Thus in D_{6h}, a $[4n+2]$ system has the following possible pairings of HOMO and LUMO:

$$\begin{aligned}
&E_{1g}^4\ E_{2u}^0 \quad E_{2u}^4\ E_{1g}^0,\\
&E_{2u}^4\ (B_{1g}+B_{2g})^0 \quad (B_{1g}+B_{2g})^4\ E_{2u}^0,\\
&E_{1g}^4\ (A_{1u}+A_{2u})^0 \quad (A_{1u}+A_{2u})^4\ E_{1g}^0
\end{aligned}$$

and $A_{2u}^2 E_{1g}^0$ for the trivial two-electron case. Only the E_{1g}, E_{2u} pairings occur for neutral D_{6h} systems, where the atom and electron count are both equal to $4n+2$ with $n = 3m+1$. The symmetry of the HOMO-LUMO product is therefore

Table 1 Symmetries of π functions of fixed angular angular momentum in the point groups D_{6h} and D_{3h}. $\Gamma(\pm k)$ is the representation of the pair of functions with quantum numbers $\pm k$ for angular momentum about the principal axis.

k	$\Gamma(\pm k)$
D_{6h}	
0	A_{1u}
$6m$	$A_{1u}+A_{2u}$
$6m\pm1$	E_{1g}
$6m\pm2$	E_{2u}
$6m\pm3$	$B_{1g}+B_{2g}$
D_{3h}	
0	A_2''
$3m$	$A_1''+A_2''$
$3m\pm1$	E''

either

$$E_{1g} \times E_{2u} = B_{1u} + B_{2u} + E_{1u}$$

or

$$E_{1g} \times (A_{1u} + A_{2u}) = E_{2u} \times (B_{1g} + B_{2g}) = 2E_{1u}$$

(and $A_{2u} \times E_{1g} = E_{1u}$ for the two-electron case), so that in every case the HOMO-LUMO excitation is translationally but not rotationally allowed (the product symmetry contains a match to the symmetry E_{1u} but not to A_{2g}).

Hence, the orbital model makes an unambiguous prediction that a strong diatropic ring current is retained in D_{6h}-symmetric geometries of [N]-annulenes with $N = 4n+2$. As the systems become larger and the π energy levels crowd together, other transitions may be expected to contribute to the description of the ring current, but these transitions will remain predominantly diatropic. In the neutral [$4n+2$] systems, for example, the first transition to have any rotational/paratropic component involves well separated orbitals whose parent angular momentum values differ by at least four. The convergence of HOMO and LUMO energies suggests that the diatropic currents will become stronger with increasing ring size.

These deductions from symmetry-adapted Hückel theory are entirely compatible with the computed pseudo-π maps for the D_{6h} geometries.

D_{3h} symmetry

In D_{3h}, the π representations are A_1'', A_2'', E'' … The functions with these symmetries can mix angular momentum components $|k|$ as:

$$\begin{aligned} A_2'' &: \quad 0,\ 3,\ 6,\ 9,\ 12,\ 15,\ \ldots \\ A_1'' &: \quad 3,\ 6,\ 9,\ 12,\ 15,\ 18,\ \ldots \\ E'' &: \quad 1,\ 2,\ 4,\ 5,\ 7,\ 8,\ \ldots \end{aligned}$$

The stack of π levels ordered by increasing node count becomes

$$\begin{aligned} &A_2'',\ E'',\ E'',\ (A_1'' + A_2''),\ E'',\ E'',\ (A_1'' + A_2''), \\ &E'',\ E'',\ (A_1'' + A_2''),\ E'',\ E'',\ \ldots \end{aligned}$$

Thus in D_{3h}, a [$4n+2$] system has the following possible pairings of HOMO and LUMO:

$$\begin{aligned} &(E'')^4\ (E'')^0, \\ &(E'')^4\ (A_1'' + A_2'')^0 \quad (A_1'' + A_2'')^4\ (E'')^0, \end{aligned}$$

(and $(A_2'')^2\ (E'')^0$ for the two-electron case). The HOMO-LUMO product symmetry is therefore either

$$E'' \times E'' = A_1' + A_2' + E'$$

(which applies to the neutral systems discussed in the present paper) or

$$E'' \times (A_1'' + A_2'') = 2'\ E'$$

(simply E' for the two-electron case). In the second case, the HOMO-LUMO transition is purely diatropic in character, as it is translationally but not rotationally allowed.

However, in the first case, which is of more interest in the present context, the HOMO-LUMO excitation is translationally and rotationally allowed, and the ring current predicted for the neutral D_{3h} systems with this HOMO/LUMO structure could in principle be of diatropic, paratropic or mixed character.

In fact, the HOMO/LUMO transition in these systems leads to a net paratropic contribution, as we have seen in the maps illustrated in Fig. 2(b). This is straightforwardly rationalised by inspecting the angular-momentum composition of the orbitals, obtained by projecting the pseudo-π molecular orbitals for the particular geometries employed here[4] onto the idealised particle-on-a-ring eigenvectors. It turns out that although the E'' HOMO pair has, as expected, a large contribution from $|k| = n$, the weight of functions with $|k| = n+1$ is almost as large. Likewise, the E'' LUMO pair contains both the expected large contribution from $|k| = n+1$ and a strong admixture of functions $|k| = n$. Rotational transitions between $\pm k$ partners induced by this mixing of different angular momenta come to dominate the contribution of the HOMO to the global ring current as the ring size increases-in [42], [54], [66]-annulenes, the HOMO contributes a strong, global, paratropic circulation (Fig. 2(b)). At the same time, the mixing of $|k| =$ n functions into the LUMO, produces a global diatropic current arising from the translational transition between the nearly degenerate ($A_1'' + A_2''$) HOMO − 1 pair and the E'' LUMO (Fig. 2(a)). Opposition of the HOMO − 1 and HOMO contributions results in loss of the global current, leaving only localised bond circulations (Fig. 2(c)).

Thus, once again the deductions from symmetry-adapted Hückel theory are entirely compatible with the computed pseudo-π maps, and furthermore, they explain in detail the reasons for the difference in magnetic aromaticity between large D_{6h} and D_{3h} [$4n+2$]-annulenes.

Conclusion

(i) Consistency of the model

This paper began from a question as to whether there was a contradiction between previous computational results[4] that indicated a loss of aromaticity for larger planar [$4n+2$]-annulenes with D_{3h} symmetry, and the ipsocentric orbital model,[11] which accounts for magnetic aromaticity in terms of symmetry-based selection rules and predicts diatropicity in [$4n+2$] monocycles with full $D_{(4n+2)h}$ symmetry.

The calculations reported here have shown that an especially economical version of the ipsocentric approach, the pseudo-π model, can be used to obtain maps of induced current density that verify the trend in the larger [$4n+2$]-annulenes to decreasing aromaticity in D_{3h}, but not D_{6h}, planar geometries. Moreover, the orbital model can account for the appearance of the computed maps in terms of simple pictorial molecular orbital theory-using only the classical concepts of symmetry and angular momentum.

It turns out that the key to the different magnetic behaviour of D_{6h} and D_{3h} geometries is the different extent of *angular momentum mixing within the frontier orbitals* allowed by the two symmetry groups. D_{6h} preserves the translational character of the HOMO–LUMO transition, whereas D_{3h} allows cancelling rotational and translational character in HOMO − 1/HOMO transitions to the LUMO.

There is therefore no conflict in interpretation of the *ab initio* computational results: aromaticity is progressively 'switched off' in the systems with lowering of symmetry, and would be further reduced with relaxation into non-planar equilibrium structures, where these turn out to be preferred for the largest systems.

The strength of the ipsocentric approach to calculation of magnetic properties, and of current density in particular, is that this approach leads not only to numerical values but, in addition, to an interpretation of the results at the orbital level.

An interesting variation on the theme of symmetry, delocalisation and steric strain is provided by the work of Kiran and Nguyen[27] in which it was shown computationally (in B3LYP/6-31G* optimisations) that symmetrical clamping of the [30]-, [42]-, [54]- and [66]-annulenes with six internal methylene bridges enhanced the stability of near-equilateral D_{6h} 'delocalised' structures. For [30] and [42] clamping brought the energy of the D_{6h} structure below that of the D_{3h} 'localised'

alternative. Magnetic properties for D_{6h} and D_{3h} structures of the modified [54] and [66]-annulenes show the same qualitative trends as found in ref. 4 for the annulenes themselves. As the angular-momentum composition of frontier orbitals is controlled by the point-group symmetry, the present work suggests that the trends in ring current behaviour of these modified systems can be expected to follow those of the parent annulenes.

(ii) A corollary for 4*n* systems

We have seen that the ipsocentric approach can explain the existing observations, but it can also answer questions about how properties would be expected to vary with electron count. As an example, what are the ring-current properties to be expected of D_{6h}/D_{3h} geometries of [4*n*]-annulenes?

Small planar [4*n*] monocycles have paratropic ring currents.[28] This is explained in the ipsocentric approach as a two-electron current arising from the rotationally allowed HOMO-LUMO transition across an angular-momentum pair split by Jahn–Teller distortion.[11] The node-counting arguments presented earlier predict that for D_{6h} and D_{3h} geometries of [4*n*]-annulenes the HOMO-LUMO pairs are A_{1u}/A_{2u} or B_{1g}/B_{2g} (D_{6h}) or A_1''/A_2'' (D_{3h}). HOMO–LUMO transitions in these systems are therefore rotationally allowed and translationally forbidden, preserving the paratropic character of the ring current contributed by the split pair. Mixing of angular momentum between HOMO and or LUMO and the immediately neighbouring orbitals is forbidden by symmetry; though transitions from HOMO − 1 to LUMO remain translationally allowed, as in smaller [4*n*] monocycles.[11] This diatropic contribution from the HOMO − 1 will be damped by the larger energy separation.

Thus, the prediction of the orbital model is that 4*n* anti-aromaticity, as defined by paratropic ring current, would persist further than [4*n* + 2] aromaticity in both D_{3h} and D_{6h} geometries of the larger annulenes, until eventually swamped by convergence of energy levels in the limit of large *n*. Support for this prediction comes from test calculations on 6+ cations of the [30] - [66]-annulenes frozen at the D_{3h} and D_{6h} geometries used for the neutral systems. All exhibit large net paratropic ring currents in their pseudo-π maps, dominated by the two-electron contribution of the HOMO. As Fig. 4 shows, this paratropic current is strong in both geometries of the cation of [30]-annulene (where it is ~4 times the benzene value). The current falls off with increasing ring size, but is still some 10–25% larger than the (diatropic) benzene current even at $N = 66$. Recent NICS calculations[29] on neutral [4*n*]-annulenes in planar conformations of lower ($D_{4h}/D_{2h}/C_s$) symmetry indicate the existence of significant paratropic ring currents; the present model explains the paratopic sense of the current in terms of the dominant rotationally allowed and translationally forbidden nature of the HOMO–LUMO transition in [4*n*] systems, which persists in all point groups that include a centre of symmetry.

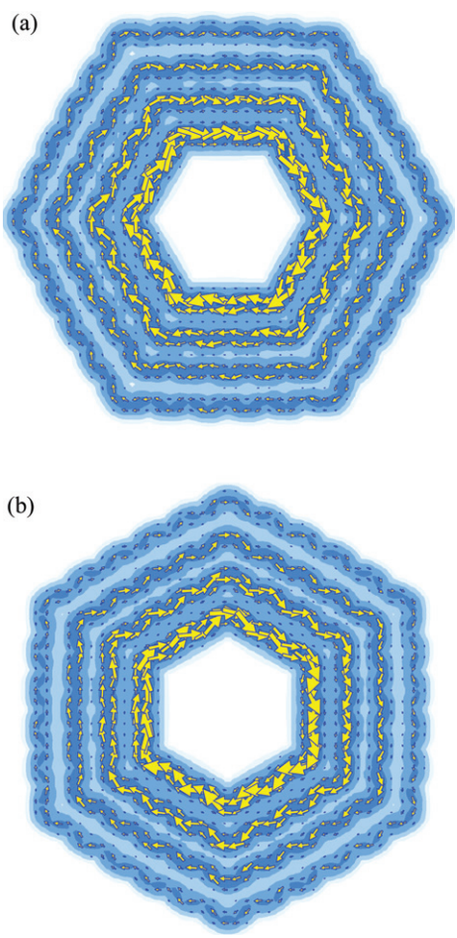

Fig. 4 Composite maps showing the paratropic π ring currents in 6+ cations of [30]-, [42]-, [54]-, [66]-annulenes arranged concentrically for ease of comparison. Currents in (a) D_{3h} (b) D_{6h} model geometries (see text). Plotting conventions and scale as in Fig. 1.

Acknowledgements

The authors acknowledge financial support from the EU Framework V programme (RTN Contract HPRN-CT-2002-00136 'WONDERFULL'), the international author travel grant programme of the Royal Society of Chemistry (0301433; L. W. J.), and the PESC subcommittee of the European Science Foundation.

References

1 H. C. Longuet-Higgins and L. Salem, *Proc. R. Soc. London, Ser. A*, 1959, **251**, 172.
2 E. Heilbronner, *J. Chem. Educ.*, 1989, **66**, 471.
3 S. Shaik, A. Shurki, D. Danovich and P. C. Hiberty, *Chem. Rev.*, 2001, **101**, 1501.
4 C. S. Wannere and P. V. R. Schleyer, *Org. Lett.*, 2003, **5**, 865, see http://pubs3.acs.org/acs/journals/supporting_information.page?in_manuscript = ol027571b.
5 K. Yoshizawa, T. Kato and T. Yamabe, *J. Phys. Chem.*, 1996, **100**, 5697.
6 (*a*) C. H. Choi and M. Kertesz, *J. Chem. Phys.*, 1998, **108**, 6681; (*b*) C. H. Choi and M. Kertesz, *J. Am. Chem. Soc.*, 1997, **119**, 11 994.
7 J. A. Pople, *Mol. Phys.*, 1958, **1**, 175.
8 J. A. Elvidge and L. M. Jackman, *J. Chem. Soc.*, 1961, 859.
9 P. v. R. Schleyer, C. Maerker, A. Dransfeld, H. J. Jiao and N. J. R. van Eikema Hommes, *J. Am. Chem. Soc.*, 1996, **118**, 6317.
10 E. Steiner and P. W. Fowler, *J. Phys. Chem. A*, 2001, **105**, 9553.
11 E. Steiner and P. W. Fowler, *Chem. Commun.*, 2001, 2220.
12 (*a*) P. W. Fowler, R. W. A. Havenith, L. W. Jenneskens, A. Soncini and E. Steiner, *Chem. Commun.*, 2001, 2386; (*b*) A. Soncini, R. W. A. Havenith, P. W. Fowler, L. W. Jenneskens and E. Steiner, *J. Org. Chem.*, 2002, **67**, 4753; (*c*) P. W. Fowler, R. W. A. Havenith, L. W. Jenneskens, A. Soncini and E. Steiner, *Angew. Chem., Int. Ed. Engl.*, 2002, **41**, 1558; (*d*) R. W. A. Havenith, P. W. Fowler and L. W. Jenneskens, *Chem. Phys. Lett.*, 2003, **367**, 468.
13 P. W. Fowler and E. Steiner, *Chem. Phys. Lett.*, 2002, **364**, 259.
14 W. Kutzelnigg, *Israel J. Chem.*, 1980, **19**, 193.
15 M. Schindler and W. Kutzelnigg, *J. Chem. Phys.*, 1982, **76**, 1919.
16 R. Ditchfield, *Mol. Phys.*, 1974, **27**, 789.
17 T. A. Keith and R. F. W. Bader, *Chem. Phys. Lett.*, 1993, **210**, 223.
18 S. Coriani, P. Lazzeretti, M. Malagoli and R. Zanasi, *Theor. Chim. Acta*, 1994, **89**, 181.
19 P. Lazzeretti and R. Zanasi, *SYSMO package*, University of Modena, 1980. Additional routines for the evaluation and

plotting of current density: E. Steiner, P. W. Fowler and R. W. A. Havenith.
20 F. London, *J. Phys. Radium*, 1937, **8**, 397.
21 G. A. Burley, P. W. Fowler, A. Soncini, J. P. B. Sandall and R. Taylor, *Chem. Comm.* In press (2003).
22 C. S. Wannere and P. v. R. Schleyer, personal communication.
23 R. C. Haddon, *J. Am. Chem. Soc.*, 1979, **101**, 1722.
24 (*a*) K. Yates, *Hückel Molecular Theory*, Academic Press, New York, 1978; (*b*) R. McWeeny, *Coulson's Valence*, Oxford University Press, Oxford, 1979.
25 A. A. Frost and B. Musulin, *J. Chem. Phys.*, 1953, **21**, 572.
26 S. L. Altmann and and P. Herzig,, *Point-Group Theory Tables*, Clarendon Press, Oxford, 1994.
27 B. Kiran and M. T. Nguyen, *Chem. Phys. Lett.*, 2001, **349**, 307.
28 H. C. Longuet-Higgins, *Paramagnetic Ring Currents in the [4n]-Annulenes, in Aromaticity*, Special Publication No. 21, The Chemical Society, London, 1967.
29 C. S. Wannere, D. Moran, N. L. Allinger, B. A. Hess, Jr., L. J. Schaad and P. V. R. Schleyer, *Org. Lett.*, 2003, **5**, 2983.

